

# One-Dimensional Models for Liquid Columns Subjected to Electric Fields

A. Castellanos<sup>1</sup>, F. J. García<sup>1</sup> and H. González<sup>1,2</sup>

**Abstract**—An analysis of slender axisymmetric liquid columns is performed on the basis of one-dimensional models, recently derived and generalized here to include the effect of dielectric forces at the interface. The natural frequencies and stability criteria in the absence of gravity are obtained. Results are compared with the known exact linear solutions of the corresponding three-dimensional problem.

## I. INTRODUCTION

THE dynamics of propagation and disintegration of liquid columns, i.e. jets and liquid bridges, has long attracted the attention of investigators. The interest in these phenomena arose not only by their beauty but also by the possibility of wide application. The solution of these problems on the basis of the general three-dimensional hydrodynamic equations involves great difficulties. We address here the question of the validity of one-dimensional models derived from appropriate truncation of the three-dimensional equations.

The linear approach shows that jets as well as cylindrical liquid bridges are unstable against axisymmetric perturbations whose wavelength is greater than the perimeter of the undisturbed column. Experimental observations also show that the breaking process is axisymmetric. This justifies considering only axisymmetric motions.

The smallness of the ratio of the radius to the initial wavelength or height of the column, allows us to obtain one-dimensional models that greatly simplify the study of these columns. The inviscid slice model introduced by Lee [1] and the Cosserat model [2], originally born in the context of continuum mechanics, are the more widely known. Here a set of one-dimensional models is derived by substituting a truncated Taylor series of the radial coordinate in the Navier-Stokes equations and boundary conditions at the interface. The Lee slice model is generalized to take account of viscosity. A new model having a parabolic radial dependence for the axial velocity is developed. The Cosserat model comes from the introduction of the mean axial velocity into the previous one, but an inconsistency arises from neglecting some viscous terms of the same order as those retained. A new model for the mean axial velocity is derived. It conserves the same inertial contribution

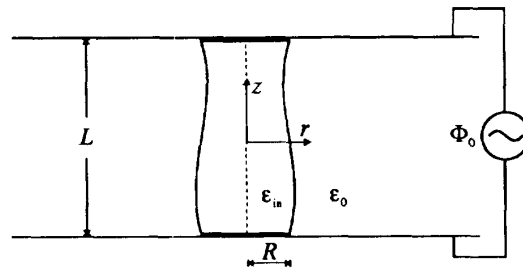


Fig. 1: Schematic description of an axisymmetric liquid bridge subjected to an a.c. axial electric field.

but avoids the above-mentioned problem by estimating the involved terms instead of neglecting them.

Electrical forces acting upon the polarization charges present at the interface increase the minimum initial wave length or height below which the column is stable. Thus, more slender columns are feasible. The derivation of one-dimensional models is generalized to include the effect of dielectric forces at the interface.

In order to test the validity of these models, a linear stability analysis is performed, first in the absence and then in the presence of the axial electric field  $E$ . It has been already shown that for jets the results obtained using these approximate models and the exact ones given by Rayleigh [3, 4] and Weber [5] are in good accordance [6]. Here the results for liquid bridges are compared to the exact linear solutions given by Sanz [7] (inviscid,  $E = 0$ ), Tsamopoulos *et al.* [8] (viscous,  $E = 0$ ), Nicolás [9] (highly viscous,  $E = 0$ ), and González *et al.* [10] (inviscid,  $E \neq 0$ ).

## II. GENERAL EQUATIONS

Let us consider a cylindrical liquid column of radius  $R$  and height  $L$  anchored between two parallel coaxial disks. The liquid is assumed to be incompressible and with constant density and viscosity (see Fig. 1). The liquid bridge, confined by surface tension, is supposed to be in a zero-gravity environment. Using the dimensional scales  $R$  for length,  $(\rho R^3/\sigma)^{1/2}$  for time,  $(\sigma/(\rho R))^{1/2}$  for velocity, and  $\sigma/R$  for pressure, the radial and axial components of the Navier-Stokes equation, and the continuity equation are

$$V_t + VV_r + WV_z = -P_r + C(V_{zz} - W_{rz}), \quad (1)$$

<sup>1</sup>Departamento de Electrónica y Electromagnetismo, Facultad de Física. Avda. Reina Mercedes s/n, 41012 Sevilla, Spain.

<sup>2</sup>Departamento de Física Aplicada, E. S. I. I., Avda. Reina Mercedes s/n, 41012 Sevilla, Spain.

This work has been supported by the Spanish Dirección General Interministerial de Ciencia y Tecnología (DGICYT) under contract PB90-0905.

$$W_t + VW_r + WW_z = -P_z + C \left( W_{zz} + W_{rr} + \frac{W_r}{r} \right), \quad (2)$$

$$\frac{1}{r}(rV)_r + W_z = 0. \quad (3)$$

where the subscripts  $t$ ,  $r$ , and  $z$  indicate derivatives with respect to time and the radial and axial coordinates, respectively; and  $V$ ,  $W$ , and  $P$  are the radial and axial velocities and pressure. The Ohnesorge number  $C = \mu/(\rho\sigma R)^{1/2}$  shows the ratio of viscous to capillary forces.

To these equations, we must add the following boundary conditions:

- Regularity at the axis and axisymmetry:

$$V(0, z, t) = 0, \quad W_r(0, z, t) = 0, \quad P_r(0, z, t) = 0; \quad (4)$$

- kinematic condition at the interface ( $r = F(z, t)$ ):

$$[F_t - V + F_z W] \Big|_{r=F(z,t)} = 0; \quad (5)$$

- normal and tangential components of the stress equilibrium at the interface:

$$P \Big|_{r=F(z,t)} = \nabla \cdot \mathbf{n} + \frac{2C}{1+F_z^2} [V_r + F_z^2 W_z - F_z(V_z + W_r)] \Big|_{r=F(z,t)}, \quad (6)$$

$$C [(W_r + V_z)(F_z^2 - 1) + 2F_z(W_z - V_r)] \Big|_{r=F(z,t)} = 0; \quad (7)$$

where  $\mathbf{n}$  is the unitary vector normal to the interface, and the mean curvature  $\nabla \cdot \mathbf{n}$ , which gives the capillary pressure, takes the form

$$\nabla \cdot \mathbf{n} = \frac{1}{(1+F_z^2)^{3/2}} \left[ \frac{1}{F} - \frac{F_{zz}}{1+F_z^2} \right]. \quad (8)$$

The above boundary conditions are valid for liquid jets as well as for liquid bridges. For the latter, some other constraints must be added in order to account for the presence of the rigid disks:

- Impenetrability of the rigid disks:

$$W(r, z = \pm\Lambda, t) = 0; \quad (9)$$

- anchoring to their respective edges:

$$F(z = \pm\Lambda, t) = 1; \quad (10)$$

- no-slip condition at the disks (if  $C \neq 0$ ):

$$V(r, z = \pm\Lambda, t) = 0; \quad (11)$$

- conservation of the volume of the liquid bridge:

$$\int_{-\Lambda}^{\Lambda} dz F^2(z, t) = \int_{-\Lambda}^{\Lambda} dz F^2(z, 0). \quad (12)$$

where  $\Lambda = L/(2R)$  is the slenderness.

The volume of the column is important for its stability properties. However, if the dynamics of the system is under study, the conservation of volume is guaranteed by fulfilment of the continuity equation (3) and the kinematic condition (5). Therefore, Eq. (12) can be considered an initial condition.

### III. ONE-DIMENSIONAL MODELS

The difficulty of the above equations can be circumvented through the use of the so-called one-dimensional models, valid for slender columns. The smallness of the typical radial length as compared to the axial one, characterized by the value  $1/\Lambda$ , suggests expanding the mentioned variables in series of powers of  $r$ . Furthermore, axisymmetry implies that the axial velocity  $W$  and the pressure  $P$  are even functions of  $r$ , while the radial velocity  $V$  is an odd one. Therefore, the following Taylor series are proposed:

$$W(r, z, t) = W_0 + \frac{1}{2}r^2W_2 + \dots + \frac{1}{(2j)!}r^{2j}W_{2j} + \dots, \quad (13)$$

$$V(r, z, t) = -\frac{1}{2}rW_{0z} - \frac{1}{8}r^3W_{2z} - \dots - \frac{2j+1}{(2j+2)!}r^{2j+1}W_{2jz} + \dots, \quad (14)$$

$$P(r, z, t) = P_0 + \frac{1}{2}r^2P_2 + \dots + \frac{1}{(2j)!}r^{2j}P_{2j} + \dots, \quad (15)$$

where the coefficients  $W_{2j}$ ,  $P_{2j}$ , with  $j = 0, 1, \dots$  are functions of  $t$  and  $z$ , and Eq. (3) is implicitly present in the series associated to  $V$ .

The generation of one-dimensional models can be summarized as follows. First, the series (13)–(15) are introduced in the momentum equations (1)–(2). This gives an infinite set of equations that can be truncated according to the relative error expected from the model. This relative error is defined as the order of magnitude of the larger neglected terms divided by that of the retained ones of the same nature. In order to characterize it, the notation  $\mathcal{O}_r(\Lambda^{-n})$  is introduced, which following an expression means that the neglected terms are of order  $1/\Lambda^n$  times the order of the retained terms. Second, the set of momentum equations is completed with the boundary conditions at the interface, in which the same Taylor series are substituted, and high-order terms are neglected consistently with the cited relative error. Finally, some of the variables can be eliminated from the formulation, providing a reduced system of differential equations which does not depend on  $r$  anymore. Since this procedure is applied to Eqs. (1)–(7), which are common to jets and bridges, the derived models are valid for both kinds of liquid columns (for details about their derivation, see [6]).

The first-order model may be called *viscous* Lee model, since in the limit  $C = 0$  it matches the inviscid slice model proposed by Lee. The relative error of this model is  $\Lambda^{-2}$ .

Since at this order the axial velocity is represented by its mean value on a slice within the same accuracy, the viscous Lee model has  $\bar{W}$  and  $F$  as variables:

$$F^2 (\bar{W}_t + \bar{W} \bar{W}_z) = -F^2 (\nabla \cdot \mathbf{n})_z + 3C (F^2 \bar{W}_z)_z, \quad (16)$$

$$(F^2)_t + (F^2 \bar{W})_z = 0. \quad (17)$$

Note that the kinematic condition (17) is exact, as it can be deduced integrating Eq. (3) on a slice.

The second-order model, with relative error  $\Lambda^{-4}$ , considers the contribution of first-order radial and axial momentum as well as second-order axial momentum equations. Since this approach leads to a parabolic radial approximation of the axial velocity, it may be called *parabolic one-dimensional model*. The subsequent system of six differential equations in the variables  $W_0$ ,  $W_2$ ,  $W_4$ ,  $F$ ,  $P_0$ , and  $P_2$  can be reduced to the following three ones for  $W_0$ ,  $W_2$ , and  $F$ :

$$F_t + \frac{1}{2} F W_{0z} + F_z W_0 + \frac{1}{8} F^3 W_{2z} + \frac{1}{2} F^2 F_z W_2 = 0, \quad (18)$$

$$\begin{aligned} (W_{0t} + W_0 W_{0z}) - \left[ \frac{1}{4} F^2 \left( W_{0tz} - \frac{1}{2} W_{0z}^2 + W_0 W_{0zz} \right) \right]_z \\ = -(\nabla \cdot \mathbf{n})_z + C \left[ 2W_{0zz} + 2W_2 - \frac{1}{4} F^2 W_{0zzz} \right. \\ \left. - F F_z W_{0zz} - \frac{1}{2} (F_z^2 + F F_{zz}) W_{0zz} + \frac{1}{4} F^2 W_{2zz} \right. \\ \left. + \frac{3}{2} F F_z W_{2z} + (F_z^2 + F F_{zz}) W_2 \right], \quad (19) \end{aligned}$$

$$\begin{aligned} F^4 \left( W_{2t} + W_0 W_{2z} + \frac{1}{2} W_{0tz} + \frac{1}{2} W_0 W_{0zz} \right) \\ = C \left( 4F^2 W_{0zz} + 24F F_z W_{0z} - 8F^2 W_2 \right. \\ \left. + \frac{1}{2} F^4 W_{0zzz} - 4F^2 F_z^2 W_{0zz} + 3F^4 W_{2zz} \right. \\ \left. + 14F^3 F_z W_{2z} + 8F^2 F_z^2 W_2 \right). \quad (20) \end{aligned}$$

The difficulty of this formulation as compared to the viscous Lee one is evident. A simpler model for the mean axial velocity and the shape of the interface can be obtained from the former. To this end, Eq. (19) multiplied by  $F^2$  is added to Eq. (20) multiplied by  $1/4$ . In this single equation,  $W_0$  can be eliminated in favor of  $\bar{W}$ . However,  $W_2$  appears in second-order viscous terms. If these are neglected, the following equation for  $\bar{W}$  and  $F$  is obtained:

$$\begin{aligned} F^2 (\bar{W}_t + \bar{W} \bar{W}_z) - \left[ \frac{1}{8} F^4 \left( \bar{W}_{tz} - \frac{1}{2} \bar{W}_z^2 + \bar{W} \bar{W}_{zz} \right) \right]_z \\ = -F^2 (\nabla \cdot \mathbf{n})_z + C \left[ 3(F^2 \bar{W}_z)_z - \frac{1}{8} F^4 \bar{W}_{zzz} \right. \end{aligned}$$

$$\begin{aligned} \left. - F^3 F_z \bar{W}_{zzz} - \frac{1}{2} (F^3 F_{zz} + 3F^2 F_z^2) \bar{W}_{zz} + \mathcal{O}_r(\Lambda^{-2}) \right] \\ + \mathcal{O}_t(\Lambda^{-4}), \quad (21) \end{aligned}$$

which together with the kinematic condition (17) constitute the well-known Cosserat one-dimensional model. The described inconsistency affects the relative error of the model, changing from  $\Lambda^{-4}$  to  $\Lambda^{-2}$  when the Ohnesorge number is large enough. This inconvenience can be overcome if Eq. (13) is substituted into Eq. (7), which allows us to obtain an approximate relationship for  $W_2$  in terms of  $\bar{W}$ . Thus, the neglected second-order viscous terms in the Cosserat model can be so estimated to give

$$\begin{aligned} F^2 (\bar{W}_t + \bar{W} \bar{W}_z) - \left[ \frac{1}{8} F^4 \left( \bar{W}_{tz} - \frac{1}{2} \bar{W}_z^2 + \bar{W} \bar{W}_{zz} \right) \right]_z \\ = -F^2 (\nabla \cdot \mathbf{n})_z + C \left[ 3(F^2 \bar{W}_z)_z \right. \\ \left. + \frac{3}{4} [(F^3 F_{zz} - 3F^2 F_z^2) \bar{W}_z]_z \right], \quad (22) \end{aligned}$$

which together with Eq. (17) is referred as the *averaged parabolic one-dimensional model*, or briefly *averaged model*. It conserves the same inertial terms as the Cosserat model, but its corrected viscous contribution guarantees that the relative error of the former is  $\Lambda^{-4}$  instead, for any value of the Ohnesorge number.

#### A. Boundary conditions at the anchoring disks.

The presence of rigid walls at  $z = \pm\Lambda$ , mathematically characterized by the boundary conditions (9)–(11), distinguishes liquid bridges from jets. The same procedure of one-dimensionalization applied to the referred conditions provides another ones that do not depend any longer on the radial variable. In order to close the problem for liquid bridges, the number of these one-dimensional boundary conditions must be the same as the differential order in  $z$  of the model.

The Lee, Cosserat, and averaged models may be called *mean-velocity models*, since all of them have  $\bar{W}$  and  $F$  as dependent variables. Their differential order in  $z$  is four for any value of  $C$ . Thus, four independent boundary conditions at the disks must be satisfied. First, the anchoring conditions (10) remain unchanged.

$$F(z = \pm\Lambda, t) = 1. \quad (23)$$

Second, as Meseguer [11] has shown, the radial integration of Eq. (9) implies that the mean axial velocity must be zero at the disks:

$$\bar{W}(z = \pm\Lambda, t) = 0. \quad (24)$$

Finally, introducing the latter conditions in the kinematic equation (17), another two conditions for  $\bar{W}$  are obtained:

$$\bar{W}_z(z = \pm\Lambda, t) = 0, \quad (25)$$

which are dependent with respect to (23).

It is important to notice that the no-slip condition (11) leads to (25) again, as can be shown by averaging Eq. (3) on a slice. Therefore, the differential order as well as the boundary conditions at the disks are independent of the value of the Ohnesorge number.

The parabolic model is defined in terms of the variables  $W_0$ ,  $W_2$ , and  $F$ . When viscosity is not zero, the differential order in  $z$  is eight, while it changes to six in the inviscid case. This imposes the number of boundary conditions in each case.

The anchoring condition at the edge of the rigid disks applies again:

$$F(z = \pm\Lambda, t) = 1. \quad (26)$$

If the series (13)–(14) are introduced in the impenetrability and no-slip conditions, (9) and (11), the following eight boundary conditions for the viscous parabolic model are obtained:

$$W_0(z = \pm\Lambda, t) = 0, \quad (27)$$

$$W_2(z = \pm\Lambda, t) = 0, \quad (28)$$

$$W_{0z}(z = \pm\Lambda, t) = 0, \quad (29)$$

$$W_{2z}(z = \pm\Lambda, t) = 0. \quad (30)$$

The four conditions (29) and (30) do not apply if  $C = 0$ . Instead substituting the above-mentioned series into the kinematic equation (18) gives another two conditions. Using (20) with  $C = 0$  to decouple  $W_2$  from the problem, the following six conditions for  $W_0$  and  $F$  must be fulfilled by the inviscid parabolic model:

$$W_0(z = \pm\Lambda, t) = 0, \quad (31)$$

$$W_{0zz}(z = \pm\Lambda, t) = 0, \quad (32)$$

$$W_{0z}(z = \pm\Lambda, t) - \frac{1}{8}W_{0zzz}(z = \pm\Lambda, t) = 0. \quad (33)$$

Conditions (33) come from imposing the anchoring of the shape of the interface to the edges of the disks. However they allow the liquid to slip on their surface, as it is expected as long as viscosity effects are absent.

Contrarily to the mean-velocity models, the parabolic one conserves the sensitivity of the general equations and boundary conditions to the viscous or inviscid character of the problem.

#### B. Presence of an axial a.c. electric field.

Consider now that an a.c. potential difference is applied to the bounding plates (electrodes) in which the liquid bridge anchors are welded (see Fig. 1). For frequencies much higher than the inverse of the charge relaxation time, the only forces of electrical origin that are of importance

are the dielectric ones. The exact formulation of the problem for static conditions has been given in [12] and for dynamic conditions in [10]. In both cases, the only place where the electric field enters the formulation of the hydrodynamic equations is in the normal stress boundary condition, where now the electric pressure has to be added to the capillary one following the substitution rule

$$\nabla \cdot \mathbf{n} \rightarrow \nabla \cdot \mathbf{n} - \Xi^2 \Delta \left[ \varepsilon \left( \frac{1}{2} \Phi_r^2 - \frac{1}{2} \Phi_z^2 - F_z \Phi_r \Phi_z \right) \right] \quad (34)$$

The Maxwell equations reduce to both the divergence and curl of the electric field being zero. Introducing the electrical potential  $\Phi$ , it must fulfill the Laplace equation

$$\nabla^2 \Phi = 0, \quad (35)$$

as well as the following boundary conditions

$$\Phi(r, z = \Lambda, t) = 1, \quad \Phi(r, z = -\Lambda, t) = 0; \quad (36)$$

$$\Phi(0, z, t) \text{ finite}, \quad (37)$$

$$\lim_{r \rightarrow \infty} \Phi(r, z, t) = \frac{z + \Lambda}{2\Lambda}, \quad (38)$$

$$\Delta \Phi = 0, \quad (39)$$

$$\Delta [\varepsilon (-\Phi_r + F_z \Phi_z)] = 0, \quad (40)$$

where  $\varepsilon$  is the ratio of the electric permittivity of the vacuum  $\varepsilon_0$  to the one of the inner liquid  $\varepsilon_{in}$ ;  $\Delta$  denotes the jump of a magnitude through the interface; and  $\Xi = (\varepsilon_{in}/(\sigma R))^{1/2} \Phi_0$  is the electric Bond number, which shows the ratio of electric to capillary forces.

#### IV. LINEAR STABILITY ANALYSIS

The static cylindrical solution is characterized by having zero velocity and constant values of the pressure and shape of the interface. A perturbative solution is proposed for the one-dimensional models, in terms of a small deviation of the amplitude of the involved magnitudes from the static solution, and second-order terms in such amplitude will be neglected. The linearized shape of the interface  $f$  becomes decoupled through the kinematic equation. The linearized one-dimensional models so obtained are valid for jets as well as for liquid bridges, and are written down explicitly in [6]. The boundary conditions at the disks for these linear mean-velocity models are given in section III.A.

A treatment similar to the one presented by González *et al.* in [10] has been performed to solve these linear boundary problems. An exponential time dependence is proposed, of the type  $e^{\Omega t}$ . The electric problem given by Eqs. (35)–(39) is solved by separation of variables. The solution takes the form of a Fourier series of sines of  $z$ . Since the electric problem is coupled to the dynamical one by the boundary conditions at the interface, the coefficients of

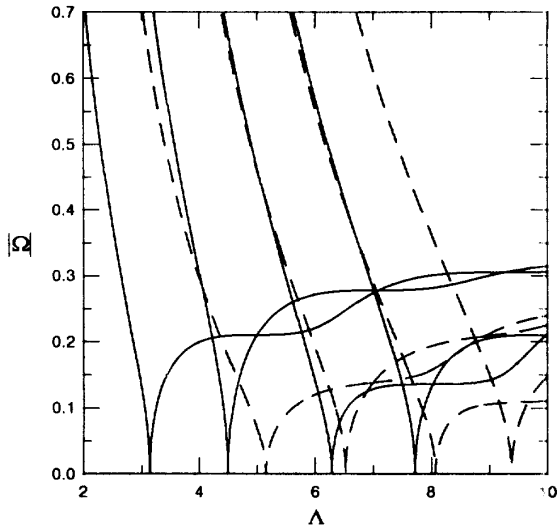


Fig. 2: Module of the eigenvalue  $\Omega$  of the first four modes as a function of the slenderness, for  $C = 0$ ,  $\varepsilon = 0.55$ ,  $\Xi = 0$  (solid) and  $\Xi = 30$  (dashed lines).

such series can be found in terms of the ones corresponding to the analogous series proposed for the velocity and the shape of the interface. The compatibility condition of the resulting system of linear equations restricts the possible values of the eigenvalue  $\Omega = \alpha + i\omega$ , whose real and imaginary part are the growth factor and the frequency of vibration of the column. The qualitative linear evolution of a liquid bridge has been well described by Meseguer [11]. For  $\omega \neq 0$  the bridge oscillates. If  $\alpha < 0$  the perturbation damps out, and if  $\alpha > 0$  it grows exponentially in time. The different resulting modes can be classified in antisymmetric or symmetric, attending to the parity of the shape of the interface for the selected mode. The first mode ( $m = 1$ ), which is antisymmetric, determines the linear stability limit.

In order to check the error of the one-dimensional models and to find the influence of the slenderness and viscosity on the evolution of the bridge, we have considered a wide range in both parameters ( $2 \leq \Lambda \leq 10$  and  $0 \leq C < \infty$ ). Notice that liquid bridges of slenderness larger than  $\pi$  are considered. The analysis of such unstable columns, not performed before, is interesting for two reasons. First, it is possible to have liquid bridges of slenderness above  $\pi$ , using either electric [12] or magnetic forces [13] to stabilize the interface, or by melting a solid metal rod passing through it an intense electric current impulse [14]. Secondly, it is interesting to predict how many drops are going to be produced in the breaking of such slender columns, as well as to determine the minimum critical length, above which these liquid bridges behave as jets.

Let  $\Lambda_s$  be the value of  $\Lambda$  for which  $\Omega = 0$ . In the inviscid case,  $\Omega$  is imaginary if  $\Lambda < \Lambda_s$ , and real otherwise. For

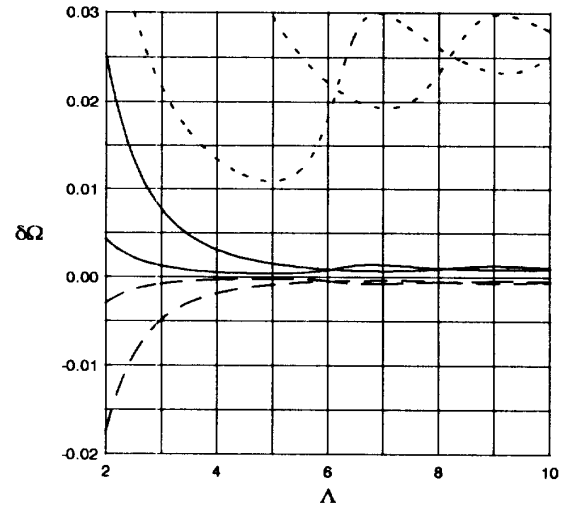


Fig. 3: Relative error in the determination of  $\Omega$  by the Lee (short dashed), Cosserat and averaged (long dashed), and parabolic (solid lines) models as a function of slenderness, for the first two modes and  $C = 0$ .

large enough viscosities,  $\Omega$  is real for any positive value of  $\Lambda$ . In Fig. 2, the module of the most significant value of  $\Omega$  is plotted against  $\Lambda$ , for the first four modes and  $C = 0$ , as calculated by Sanz [7]. These data and the ones provided by Nicolás [9], have been used to calculate the relative errors in the eigenvalue given by the Lee, Cosserat, averaged and parabolic models, which are plotted in Figs. 3 and 4. Such deviations are respectively related to the neglected inertial and viscous terms in the derivation of these models. These results can be compared to the respective ones for jets [3, 4, 5], by taking  $k = m\pi/\Lambda$  as the dimensionless wavenumber, where  $m$  characterizes the selected mode.

Notice that, for  $\Lambda > \Lambda_s$  and  $C = 0$ , the growth factor as well as its relative error do not tend to zero, but to a constant value that is common to all modes. This can be explained in terms of a characteristic nondimensional axial length  $\lambda$ , defined as the distance between consecutive nodes of the shape of the interface.  $\lambda$  is a half of the wavelength in a jet, but does not necessarily coincide with  $\Lambda$  for slender enough bridges. Let  $\lambda_{\max}$  be the value of  $\lambda$  for which the maximum growth factor is attained in a jet, which is about 4.51 in the inviscid case. In a bridge and for a given value of  $\Lambda$ , the most unstable mode should have a similar value of  $\lambda$ . However, the latter can never be greater than  $\Lambda$ , which shows that the slenderness can be considered a good measure of the characteristic axial length if  $\Lambda < \lambda_{\max}$  (for  $m=1$ ). For more slender bridges, it is expected that  $\lambda \simeq \lambda_{\max}$ , independently of the value of  $\Lambda$ , and new nodes appear in the shape of the interface. In fact, this is observed in Fig. 5, where the shape of the interface is plotted against  $z/\Lambda$  for increasing values of  $\Lambda$ ,  $C = 0$ , and  $m=1$ . For a given mode  $m$ ,  $\lambda_m$  is approximately given by

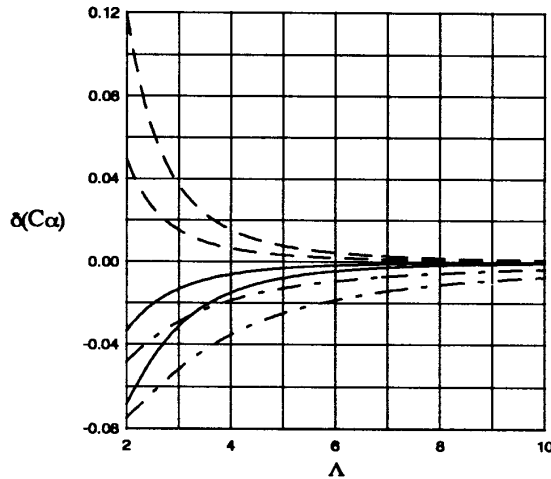


Fig. 4: Relative error in the determination of  $C\alpha$  by the Lee and averaged (long dashed), Cosserat (dotted-dashed), and parabolic (solid lines) models as a function of slenderness, for the first two modes and  $C \gg 1$ .

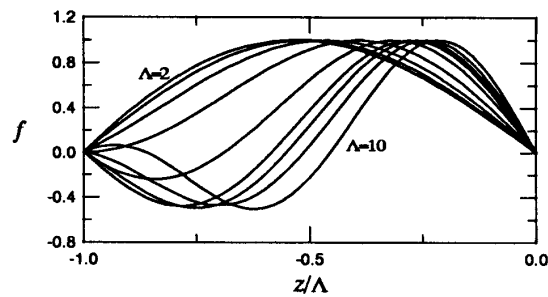


Fig. 5: Shape of the interface of the first antisymmetric mode versus  $z/\Lambda$ , for  $C = 0$  and  $\Lambda = 2, 3, \dots, 10$ , as given by Sanz.

$$\lambda_m \simeq \begin{cases} \frac{2\Lambda}{m+1} & (\text{if } \Lambda < \frac{m+1}{2}\lambda_{\max}), \\ \lambda_{\max} & (\text{if } \Lambda > \frac{m+1}{2}\lambda_{\max}). \end{cases} \quad (41)$$

Since the typical axial length is responsible for the relative error of the one-dimensional models, this one remains approximately constant for large enough  $\Lambda$ . Concerning the influence of viscosity,  $\lambda_{\max}$  increases as  $C$  does. Thus, the value of  $\Lambda$  for which new nodes appear increases, and  $\lambda \simeq \Lambda$  if  $C \gg 1$ , for any value of  $\Lambda$ . This fact is put in evidence in Fig. 6, where the shape of the interface is plotted for several values of  $C$ , as given by the parabolic model, the other models giving very similar results. This explains the clear analogy between very viscous liquid jets and bridges observed by Nicolás [9], and why the relative error of one-dimensional models tends to zero as  $\Lambda \rightarrow \infty$  for  $C \gg 1$ .

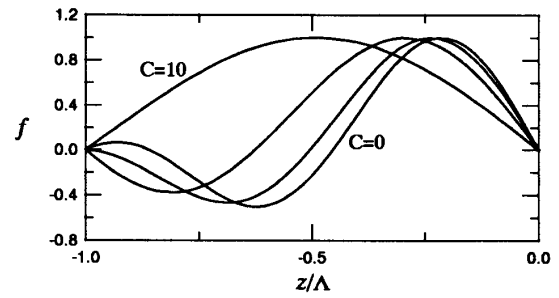


Fig. 6: Shape of the interface of the first antisymmetric mode versus  $z/\Lambda$ , for  $C = 0, 0.1, 1, 10$ , and  $\Lambda = 10$ , as given by the parabolic model.

The main features discussed in the derivation of the one-dimensional models arise in Figs. 3 and 4. If  $C = 0$ , the Cosserat and averaged models coincide. Their error is of the same order than the one of the parabolic model, as expected. The error of the Lee model is about twenty times greater than the previous ones. Although the linear Lee model tends to coincide with the averaged one when  $C \rightarrow \infty$ , this is not true when nonlinear terms are taken into account. Therefore, the good behavior of the former cannot be extended to more realistic situations. In this limit, the Cosserat model exhibits a worse agreement with the exact solution, due to the inconsistency in the second-order viscous terms. The better results of the averaged model get worse for  $\Lambda < 2$ , since the approximation of the terms neglected by the Cosserat one is not so good for small slenderness. Concerning the parabolic model, the error in the first two modes does not overcome a 7% in the studied parametric range. As expected, the error increases with the index of the mode, due to the decreasing typical axial length.

Mesguer [11] has carried out a study of the dependence of  $\Omega$  on  $\Lambda$  for several values of  $C$ , by means of the Cosserat model. Quite similar results are obtained with the other models above derived. A comparison to the exact linear results of Tsamopoulos *et al.* [8] is not interesting, since most of these are given for small values of the slenderness. However, relative errors can be calculated for  $\Lambda = 10\pi/9$  and  $2\pi/3$ , with  $C = 0.1$ . For the first data ( $\Lambda \simeq 3.50$ ), the errors of the Lee, Cosserat, averaged and parabolic models are respectively 0.6%, 0.3%, 0.09%, and 0.095%; and for the second value ( $\Lambda \simeq 2.09$ ) we have 3.1%, 0.5%, 0.6%, and 0.6%. The former data show the inconsistency in the viscous terms of the Cosserat one, even for such a small value of  $C$ , and are in qualitative accordance with the corresponding results for  $C \gg 1$ . Notice that, as García and Castellanos have shown for jets, the weight of the viscous terms can be large for relatively small viscosities, provided  $|\Omega|$  is small enough.

In Fig. 2 the module of the eigenvalue is plotted against  $\Lambda$ , for  $\varepsilon = 0.55$ ,  $\Xi = 30$ , and  $C = 0$ . Notice that the value of  $\Lambda$  for which the bridge becomes unstable increases

## V. CONCLUSIONS

A set of new one-dimensional models for viscous jets, recently developed, has been generalized to include the anchorage to rigid disks and the effect of dielectric forces. A linear stability analysis based on these models has been performed. For a given value of the viscosity, there is a value of the slenderness above which the liquid bridges tend to behave as jets. It can be concluded from the comparison with the known exact three-dimensional linear solutions that the one-dimensional models are quite adequate to deal with the first stages of development of perturbations. The accuracy of these models improves in the presence of an a.c. axial electric field, since the latter makes the typical axial length increase.

## REFERENCES

- [1] H. C. Lee, "Drop formation in a liquid jet," *IBM J. Res. Develop.*, vol. 18, pp. 364-369, 1974.
- [2] A. E. Green, "On the nonlinear behavior of fluid jets," *Int. J. Eng. Sci.*, vol. 14, pp. 49-63, 1976.
- [3] Lord Rayleigh, "On the instability of jets," *Proc. Lond. Math. Soc.*, vol. 10, pp. 4-13, 1878.
- [4] Lord Rayleigh, "On the instability of a cylinder of viscous liquid under capillary forces," *Philos. Mag.*, vol. 34, pp. 145, 1892.
- [5] C. Weber, "Zum Zerfall eines Flüssigkeitsstrahles," *Z. Angew. Math. Mech.*, vol. 11, pp. 136-154, 1931.
- [6] F. J. García and A. Castellanos, "One-dimensional models for slender axisymmetric viscous liquid jets," *Phys. Fluids*, August 1994.
- [7] A. Sanz, "The influence of the outer bath in the dynamics of axisymmetric liquid bridges," *J. Fluid Mech.*, vol. 156, pp. 101-140, 1985.
- [8] J. Tsamopoulos, T. Y. Chen, and A. Borkar, "Viscous oscillations of capillary bridges," *J. Fluid Mech.*, vol. 235, pp. 579-609, 1992.
- [9] J. A. Nicolás, "Hydrodynamic stability of high-viscosity cylindrical liquid bridges," *Phys. Fluids A*, vol. 4, pp. 1620-1626, 1992.
- [10] H. González, A. Castellanos, A. McCluskey, and F. M. Gañán, "Small oscillations of liquid bridges subjected to a.c. fields," in *Synergetics, Order and Chaos*. World Scientific, Singapore, 1988.
- [11] J. Meseguer, "The breaking of axisymmetric slender liquid bridges," *J. Fluid Mech.*, vol. 130, pp. 123-151, 1983.
- [12] H. González, F. M. J. McCluskey, A. Castellanos, and A. Barro, "Stabilization of dielectric liquid bridges by electric fields in the absence of gravity," *J. Fluid Mech.*, vol. 206, pp. 545-561, 1989.
- [13] A. Castellanos and H. González, "Stability of inviscid conducting liquid columns subjected to a.c. axial magnetic fields," *J. Fluid Mech.*, vol. 265, pp. 245-263, 1994.
- [14] C-Y. Chow and M. Harvanek, "Electromagnetic-capillary instabilities of liquid cylinder: production of spherical shells in microgravity," *AIAA J.*, vol. 28, no. 2, pp. 372-374, February 1990.

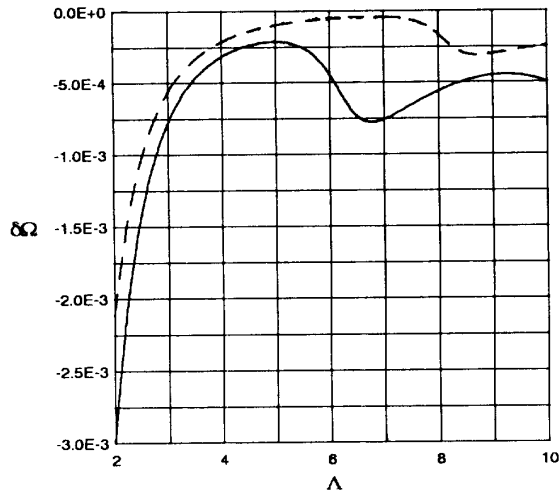


Fig. 7: Relative error in the determination of  $\Omega$  by the Cosserat and averaged models as a function of slenderness, for the first mode,  $C = 0$ ,  $\varepsilon = 0.55$ ,  $\Xi = 0$  (solid), and  $\Xi = 30$  (dashed line).

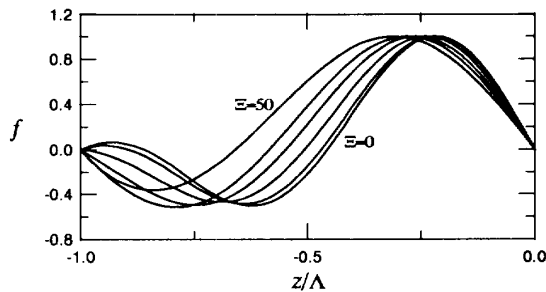


Fig. 8: Shape of the interface of the first antisymmetric mode versus  $z/\Lambda$ , for  $C = 0$  and  $\Xi = 0, 10, 20, 30, 40, 50$ , as given by González *et al.*

as the electric field increases, as shown by González *et al.* [12]. The effect of viscosity is attenuated by the presence of the electric field, i.e. for the same value of  $C$ ,  $\omega$  increases (if the bridge is stable) and  $\alpha$  decreases, as  $\Xi$  increases. The corresponding relative errors of the Cosserat and averaged models for the first mode are shown in Fig. 7. It is observed that the relative errors decrease as the electric field increases. The stabilizing effect of the electric field makes the typical axial length increase, as can be observed in Fig. 8, where the shape of the interface is shown for  $\Lambda = 10$ ,  $C = 0$ ,  $\varepsilon = 0.55$ , and several values of  $\Xi$ . Therefore, the above one-dimensional models are expected to behave even better when an axial electric field is applied.